PCCP

ROYAL SOCIETY OF CHEMISTRY

PAPER

View Article Online
View Journal

Cite this: DOI: 10.1039/d5cp04244e

Conformational studies of 1,2-di-*tert*-butoxyethane with special attention to the *gauche* oxygen effect

Hidemine Furuya, *[a] Takahiro Takekiyo, [b] Ryoichi Wada, [c] Kunihiro Kasezawa, [c] Akihiro Abe [d] and Minoru Kato [c]

Polyoxyethylene and its derivatives are highly soluble in both water and conventional organic solvents, and are widely used for many applications. Their usefulness is largely due to the ethylene glycol (EG) unit that makes up the chain. In order to understand the unique properties of the chain, many studies have been reported on its monomeric model compound, 1,2-dimethoxyethane (DME). We have attempted to study how substitution of the terminal methyl by bulky nonpolar groups affects the through-space 1,5-interaction and consequently the *gauche* oxygen effect of the central C–C bond. Conformational analysis of 1,2-di-*tert*-butoxyethane (DTBE, X–OCH_2–CH_2O–X with X = *t*-butyl) was carried out using Raman spectroscopy, with supplementary use of NMR and quantum chemical calculations. Introduction of the *t*-butyl groups should largely enhance the hydrophobicity of the molecular environment, yet DTBE was found to be soluble in water. While bond rotations around the terminal X–O bonds are significantly constrained, the *gauche* preference around the central C–C bond was found to be less affected. While electrostatic interactions play an important role in the non-hydrogen-bonding media, hydrogen-bonding comes into play in the solvents capable of forming intermolecular hydrogen-bonds. Unexpectedly, some observable amount of the through-space 1,5-*t*-Bu···O contact characteristic of the *tgg′* conformation was detected in DTBE in the gas phase. Unlike DME, however, such electrostatic attractions are completely suppressed in the condensed phase. These results indicate that the *gauche* oxygen effect of EG units is not necessarily related to the through-space 1,5-contact involving adjacent C–O bonds.

Received 4th November 2025,
Accepted 13th February 2026

DOI: 10.1039/d5cp04244e

rsc.li/pccp

1. Introduction

A vast amount of effort has made it clear that the unique characteristics of polyoxyethylene (POE) are essentially due to the specific arrangement of ether oxygens along the backbone.[1–19] While POE is highly soluble in various organic solvents of different polarities, it also dissolves well in water. Since similar rotational characteristics are inherent in 1,2-dimethoxyethane, X–OCH_2–CH_2O–X with X = CH_3 (DME), the simplest model compound of the POE chain, the molecule has attracted interest of many researchers. Among them, Matsuura *et al.*'s exploratory effort[4–13] using vibrational spectroscopy is worth mentioning. Based on the results of thermodynamic analysis, Wada *et al.*[14] concluded that the shift in conformational equilibrium is largely responsible for the high solubility of DME in water. Knowledge gained through these multifaceted studies on DME has helped in elucidating the conformational properties of POE and related systems.[15–19]

Since Morino and coworkers[20] revealed the existence of rotational isomerism in 1,2-dichloroethane (DCE) using electron diffraction, a tremendous amount of research has been conducted on the rotational behaviors of C–C bonds with related arrangements.[21] It is known that when there are highly electronegative atoms on both ends of ethane, the *gauche* state tends to become stable around the C–C bond and more so in polar media in reflecting the difference in polarity of the *gauche* and *trans* arrangements. A typical example is 1,2-difluoroethane. Wolfe[22] named these phenomena the *gauche* effect. A similar tendency exhibited by the ethylene glycol (EG) moiety (–OC–CO–) is sometimes called the *gauche* oxygen effect. For DME, it has been confirmed that the *gauche* form tends to be more stable in both liquid[23–25] and crystalline state.[23,26] In the gaseous state, on the contrary, the *trans* form becomes

[a] School of Materials and Chemical Technology, Institute of Science Tokyo, 2-12-1-S8-29 Ookayama, Meguro-ku, Tokyo 152-8550, Japan. E-mail: furuya@mct.isct.ac.jp
[b] Depeartment of Applied Chemistry, National Defense Academy, 1-10-20, Hashirimizu, Yokosuka, Kanagawa, 239-8686, Japan
[c] Department of Applied Chemistry, Graduate School of Life Sciences, Ritsumeikan University, 1-1-1 Nojihigashi, Kusatsu, Shiga 525-8577, Japan
[d] Professor Emeritus, Institute of Science Tokyo, 2-12-1 Ookayama, Meguro-ku, Tokyo 152-8550, Japan

dominant.[6,27–29] DME has two additional backbone chains and thus nine possible conformers. A significant amount of *tgg′* conformers was found to exist in the gaseous state.[27–29] This is an arrangement that occurs when the central C–C bond and the adjacent O–C bond have opposite *gauche* rotations. An explanation offered is such that the intramolecular hydrogen-bond formed between CH_3 and O situated at the 1,5-position overcomes steric repulsions inherent to the arrangement. Such a through-space 1,5-contact tends to be largely suppressed in the liquid state.[30,31]

Unlike in the case of DCE, in DME, the intramolecular rotation of the terminal C–O bonds may also play some important role in the *gauche* effect. From this perspective, we here attempted to examine how replacing the terminal methyl group with bulky nonpolar substituents affects the conformational diversity arising from the neighbor-dependent characteristic of bond rotations:[32] in short, suppression of *gauche* rotation about the C–O bond would markedly destabilize the *tgg′* conformation, thereby allowing the *gauche* oxygen effect of the central C–C bond to be examined without the influence of 1,5-through space interactions. In parallel, another motivation is how such modification affects solvation behaviors of the molecule in polar solvents including water. 1,2-Di-*tert*-butoxyethane, X–OCH_2–CH_2O–X with X = *t*-butyl (DTBE) was chosen for this purpose. Representative spatial configurations of DTBE are depicted in Fig. 1. The steric and electronic effects brought about by the introduction of the bulky *t*-butyl group will be discussed in detail in the text.

In this study, conformational analysis of DTBE was carried out using Raman spectroscopy, with supplementary use of NMR and molecular orbital (MO) calculations. To facilitate the presentation, some experimental results, such as Raman spectrum assignments and results of the NMR analysis and the MO calculation, are included in the experimental section.

2. Experimental section

2-1. Synthesis of DTBE and sample preparation

DTBE was prepared by an etherification of 2-*tert*-butoxyethanol with isobutene in the presence of H_2SO_4 and purification by vacuum distillation at 335 K and 15 mmHg.

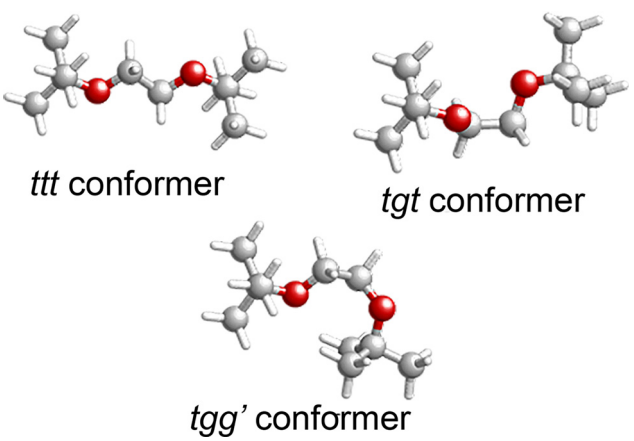

Fig. 1 Three major conformers of DTBE.

As for solvents, cyclopentane (>98%, Tokyo Chemical Industry Co., Ltd), cyclohexane (>99.5%, Tokyo Chemical Industry Co., Ltd), diethyl ether (>99.5%, Wako Pure Chemical Ind. Ltd), 1-bromopropane (>98%, Tokyo Chemical Industry Co., Ltd), ethanol (>99.5%, Wako Pure Chemical Ind. Ltd), dimethylformamide (>98%, Tokyo Chemical Industry Co., Ltd), methanol (>99.8%, Tokyo Chemical Industry Co., Ltd), ethylene glycol (>99%, Tokyo Chemical Industry Co., Ltd), and distillated water were used without further purification.

2-2. Raman spectroscopy – assignment of the observed Raman bands

Raman spectra were measured using a NR-1800 Raman spectrophotometer (JASCO, Tokyo, Japan) equipped with a single filter polychromator and a liquid nitrogen cooled CCD detector. The spectral resolution was 7.0 cm^{-1}. The 514.5 nm line from an Ar^+ laser (Spectra Physics Co.) was used with a power of 350 mW at the sample. The scattering light was measured at an angle of 90° relative to the exciting laser beam. For gas-phase spectral measurements, a flask containing DTBE (5–10 mL) and a sealed quartz cell equipped with a stopcock were connected to a vacuum line, and the pressure was reduced to 100 Pa. The flask was subsequently heated to 323 K, and the resulting DTBE vapor was collected in a sealed quartz cell. The Raman spectrum of gaseous DTBE was recorded at 298 K. The exposure time was 90 s, and the spectrum was accumulated five times. For measurements in the condensed phase, the exposure time was 300 s, and the spectrum was accumulated twice. The temperature of the samples was maintained within ±0.3 K by circulating thermostated water around the cell. All Raman spectral lines were fitted with the Gaussian–Lorentzian mixing functions using GRAMS/386 software (Galactic Industries Co.). The concentration (mole fraction) of the samples subjected to observation was 0.02 for all solvents. Temperature was kept constant at 298 K unless otherwise noted. All the measurements were carried out under atmospheric pressure.

Geometric optimizations of DTBE conformers were conducted at the B3LYP/6-31G(d,p) level using the GAUSSIAN 09 program,[33] followed by frequency calculations at the same level. The computed vibrational frequencies were scaled by a factor of 0.978, which was determined by comparing the calculated and experimental Raman spectra of DTBE in the gas phase.

Examples of the Raman spectra of DTBE in the region from 650 to 830 cm^{-1} are shown in Fig. 2 in the order (a) the neat liquid and (b) the gas phase. The observed bands are due to hybridization of the CH_3 rocking, COC bending and CH_2 rocking modes, and they are strong and respectively arise from the *ttt*, *tgt* + *tgg′*, and *tgg′* conformers. The frequencies calculated in this region (Fig. 2c) are well consistent with the observed gas-phase frequencies (Fig. 2b). The vibrational assignments of conformers adopted in this work are indicated in the diagram. In water, the intensities of the Raman spectra appreciably vary with temperature: representative examples are shown in Fig. 2d.

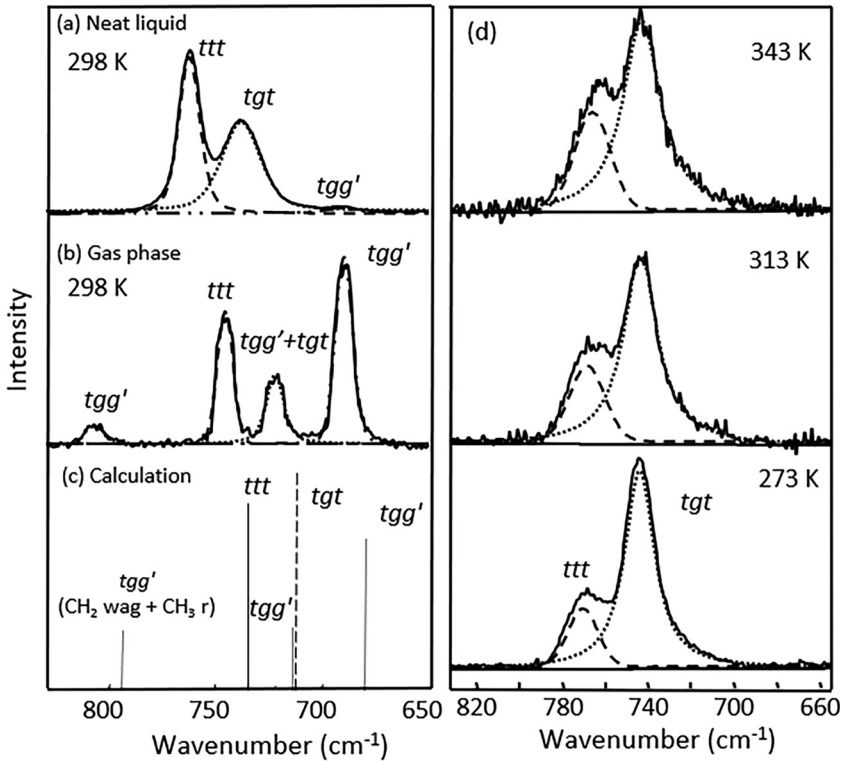

Fig. 2 Raman spectra of DTBE in the region from 650 to 830 cm^{-1}: (a) neat, (b) gas, and (c) DFT calculation. Additionally, (d) thermal variation of the Raman spectra of DTBE in water.

2-3. NMR coupling constant measurements

^{1}H- and ^{13}C-NMR spectra were recorded on a JEOL GSX-500 spectrometer operating at 500 and 125 MHz, respectively. The measurements were carried out under nearly the same conditions as those adopted in the previous conformational analysis of DME.[25] The three vicinal coupling constants $^3J_{HH}$ and $^3J'_{HH}$ for the C–C bond and $^3J_{CH}$ for the neighboring C–O bond (*cf.* Fig. 3) were measured in cyclohexane and acetonitrile (5 v/v%) at various temperatures. The analysis was carried out according to the following scheme.

Assuming $J_t = J'_t$ and $J_g = J'_g = J''_g$, the observed $^3J_{HH}$ and $^3J'_{HH}$ can be expressed as

$$^3J_{HH} = J_g f_t^{CC} + (1/2)(J_t + J_g) f_g^{CC} \quad (1)$$

and

$$^3J'_{HH} = J_t f_t^{CC} + J_g f_g^{CC} \quad (2)$$

where f_t^{CC} and f_g^{CC} ($= 1 - f_t^{CC}$) respectively denote fractions of the *trans* and *gauche* conformer around the central C–C bond (Fig. 3a). In this study, while the *trans* coupling J_t was set equal to 11.7 Hz,[31] the corresponding J_g values were somewhat adjusted to improve the fitting with the observed temperature dependence of $^3J_{HH}$ and $^3J'_{HH}$: J_g = 3.99 Hz (in cyclohexane) and 2.99 Hz (in acetonitrile).

We also measured the vicinal coupling constants $^3J_{CH}$ from the proton-coupled ^{13}C spectra for the terminal ether group ^{13}C(*t*-Bu)O–CH(^{1}H)–.

$$^3J_{CH} = J_g f_t^{CO} + (1/2)\left(J_t + J'_g\right) f_g^{CO} \quad (3)$$

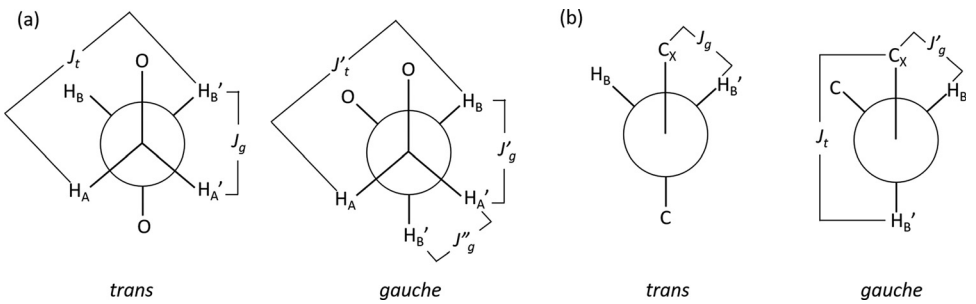

Fig. 3 (a) Definition of the *trans* and *gauche* vicinal ^{1}H–^{1}H couplings around the C–C bond. (b) The ^{13}C–^{1}H couplings for the C–O bond.

where f_t^{CO} and f_g^{CO} respectively denote fractions of the *trans* and *gauche* arrangement for the C–O bond (Fig. 3b). Following the previous treatment of DME,[31] we set J_g = 2.0 Hz and $J_t + J'_g$ = 16.0 Hz for the ^{13}C–^{1}H couplings around the C–O bond.

In the rotational isomeric state (RIS) scheme, the fraction of a given conformer is expressed by a sum of the statistical weights assigned to the individual intermolecular interactions. Each statistical weight may be related to the corresponding conformational energy (ΔE) by the Boltzmann relationship. The first-order interactions associated with the *gauche* rotation around the C–C and C–O bond are respectively represented by assigning the statistical weight σ and ρ, the weight of unity being assigned to the *trans* state. The higher order interaction involved in the *tgg′* arrangement is expressed by ω. Since bond rotations are neighbor-dependent within the chain, elucidation of the best-fit set of conformers requires a somewhat elaborate procedure.

As before,[25] simulations were performed to satisfy eqn (1)–(3). The results are compared with those observed for cyclohexane and acetonitrile, respectively, in Fig. 4a and b. The best-fit set of ΔE values estimated for the individual conformers by simulation are summarized in Table 1.

During the iterative simulation process, the thermal variation of the observed coupling constants was found to be quite insensitive to ω in the range $\Delta E_\omega > 0.5$ kcal mol^{-1}. In Table 2, the value of ΔE_ω is set equal to 0.5 kcal mol^{-1} so as to be consistent with the results of MO calculations (see later). NMR studies provide information about the rotation around the C–O bond next to the central C–C bond. The analysis suggests that the *gauche* state of the C–O bond is more than 2 kcal mol^{-1} higher than the *trans* state in the DTBE system. This result indicates that the rotational energy around the C–O bond ΔE_ρ increased by approximately 1 kcal mol^{-1} by replacing the terminal methyl with a *t*-butyl group.[3]

Table 1 Conformational energies ΔE_{tgt} and ΔE_{ttg} respectively deduced for the rotation around the C–C and C–O bonds from the NMR coupling constant measurements in cyclohexane and acetonitrile. The through-space 1,5-interaction associated with the *tgg′* arrangement is known to be almost nil in the liquid phase (see Fig. 2)

Solvent	ΔE_{tgt}[a] (ΔE_σ)	ΔE_{ttg}[a] (ΔE_ρ)	ΔE_ω[b]
Cyclohexane	−0.38	2.3	0.5
Acetonitrile	−0.76	2.1	0.5

[a] Energies expressed relative to the *ttt* state. [b] Interaction energy due to the 1,5-through space contact between the *t*-butyl group and O atom associated with the *tgg′* arrangement (for details, see a later section).

Table 2 Theoretical estimation of free energy differences ΔG (kcal mol^{-1}) for DTBE conformers in the gas phase and some representative solvents using the CCSD(T)/Def2-TZVPPD set[a]. The values are expressed relative to those of the *ttt* state. The dielectric constants (ε) of the media are also included

	Gas	Cyclohexane	Acetonitrile	Water
ε	1.0	2.02	35.6	78.5
ttt	0.00	0.00	0.00	0.00
tgt	1.27	0.13	−0.58	−0.72
tgg′	3.05	2.70	2.83	2.82

[a] For estimation of the ΔG term, the MP2/Def2-TZVPPD set was used to elucidate the entropy contribution. The polarizable continuum model (PCM) was employed to evaluate solvent effects.

2-4. *Ab initio* MO calculations using the CCSD(T) method

In attempting to perform MO calculations on DTBE, various techniques were examined, including DFT and *ab initio* theories. The effect of solvation on the conformational energies was studied on the TSUBAME4.0 supercomputer at the Institute of Science Tokyo and a supercomputer at the Research Center for Computational Science. The obtained results were largely scattered depending on the basis set used. The greatest discrepancy was found in the free energy calculation for the *tgt*

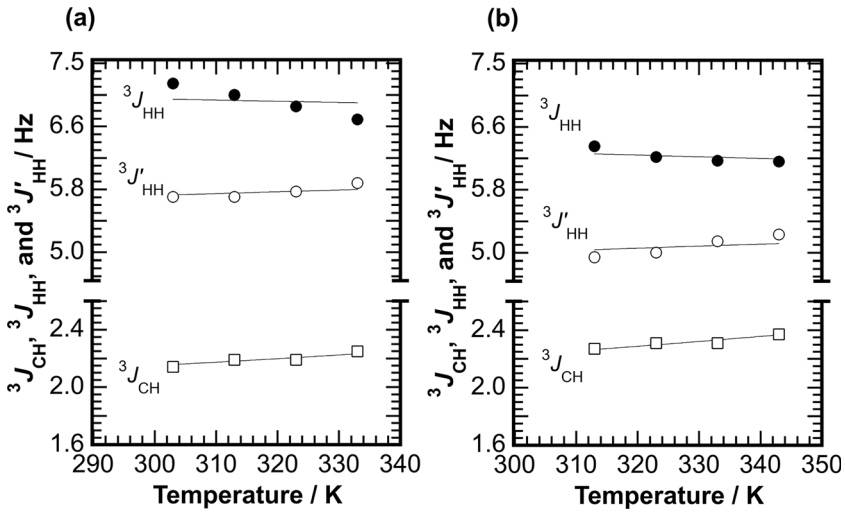

Fig. 4 Temperature dependence of ^{1}H–^{1}H vicinal couplings for the C–C bond ($^3J_{HH}$ and $^3J'_{HH}$) and the ^{13}C–^{1}H couplings for the C–O bond ($^3J_{CH}$) in (a) cyclohexane and (b) acetonitrile.

and *ttt* conformers in the gas phase. The difference ΔG varies over a wide range from negative to positive depending on the basis set employed.

The MO calculations using the CCSD(T) method[34] with the Def2-TZVPPD basis set[35] were costly, but found to yield reasonably consistent results with the experimental observation. The values of the free energy difference ΔG elucidated for *ttt*, *tgg*, and *tgg′* conformers of DTBE are accommodated in Table 2.

3. Results and discussion

3-1. *Gauche* oxygen effect of the EG moiety in solution

The multiplicities of conformers are *ttt*(1), *tgt*(2), and *tgg′*(4). Although the presence of the *tgg′* conformer is noticeable in the Raman spectrum in the gas phase, it becomes hardly detectable in liquid or in solution (*cf.* Fig. 2). In the condensed phase, therefore, the band at 730 cm^{-1} in the Raman spectra should mostly originate from the *tgt* conformer. The band at 760 cm^{-1} solely consists of the contribution of the *ttt* conformer in both phases.

The observed Raman band intensity (I) is proportional to the product of the Raman cross section (σ) and the concentration of the conformer (c):[36] $I \propto \sigma c$. The spectral intensities obtained for the major conformers, I_{ttt}, I_{tgt}, and $I_{tgg'}$, were used to define the intensity fraction. Although on the fractional basis, the order is *tgg′*, *tgt*, *ttt* in the gas phase, when multiplicity, *i.e.*, *ttt*(1), *tgt*(2) and *tgg′*(4), is taken into account, the non-polar *ttt* becomes the most stable, and the energy levels of *tgg′* and *tgt* are higher in the range of 0.5–0.6 kcal mol^{-1}. As shown in Fig. 5a, the *tgt* form increases rapidly as a function of dielectric constant (ε) of the surrounding media and becomes dominant above $\varepsilon \sim 5$ (for ε of the individual solvents, see Table 3). In contrast, the fraction of *tgg′* decreases sharply with ε, and in cyclopentane (ε = 1.97), only a trace amount is detected. Shown in Fig. 5b is the plot of ln (I_{tgt}/I_{ttt}) against ε. The variation of $\ln(I_{tgt}/I_{ttt})$ reflects the shift of the Gibbs free energy difference between the two conformers, *ttt* and *tgt*. The trajectory of the data points implies that the curve consists of two different contributions. In the figure, solvents capable of forming hydrogen-bonds (○) and those lacking such ability (●) are shown separately. They seem to lie on straight lines with different slopes.

Table 3 Enthalpy differences ΔH_{tgt} between the *tgt* and *ttt* conformers of DTBE in various solvents, due to Raman spectroscopy. For the purpose of later discussion, solvation enthalpies ΔH_{tgt}^{solv} calculated by IEFPCM are also included

Solvent	ε	ΔH_{tgt} (kcal mol^{-1}) (*a*)	ΔH_{tgt}^{solv} (kcal mol^{-1}) (*b*)	(*a*) − (*b*) (kcal mol^{-1})
Cyclopentane	1.97	1.00 ± 0.17	0.54	0.46
Diethyl ether	4.24	0.88 ± 0.12	0.33	0.55
Neat	~7[a]	0.74 ± 0.10	0.19	0.55
1-Bromopropane	8.05	0.60 ± 0.07	0.16	0.44
Ethanol	24.3	0.02 ± 0.05	−0.05	0.07
Methanol	32.6	−0.24 ± 0.02	−0.09	−0.15
DMF	38.3	0.29 ± 0.07	−0.10	0.39
Ethylene glycol	41.1	−0.33 ± 0.02	−0.11	−0.22
Water	78.5	−1.82 ± 0.12	−0.15	−1.67

[a] The observed value is not available. Listed is an estimated value from DME.

The enthalpy difference ΔH_{tgt} between the *tgt* and *ttt* states can be determined, in accordance with a standard method, from the temperature dependence of the intensity ratio I_{tgt}/I_{ttt}:

$$-\frac{\Delta H_{tgt}}{R} = \frac{\partial \ln(I_{tgt}/I_{ttt})}{\partial(1/T)} \quad (4)$$

where R and T denote the gas constant and temperature, respectively. As in most precedents, we assume that the ratio $\sigma_{ttt}/\sigma_{tgt}$ is independent of temperature. All the measurements were carried out under atmospheric pressure over the temperature range of 273 to 343 K.

The values of ΔH_{tgt} thus derived are listed in the 3rd column of Table 3, together with the ε values of the solvent (2nd column). As with DME, the value of ΔH_{tgt} is affected considerably by the nature of the solvent. In Fig. 6, ΔH_{tgt} values are plotted against ε, together with those derived from the NMR coupling constant analysis (ΔE) (Table 1), and the results of theoretical calculation by the CCSD(T)/Def2-TZVPPD method (ΔG) (Table 2). The terminology used for energy parameters differs depending on how they were determined (see the preceding section).

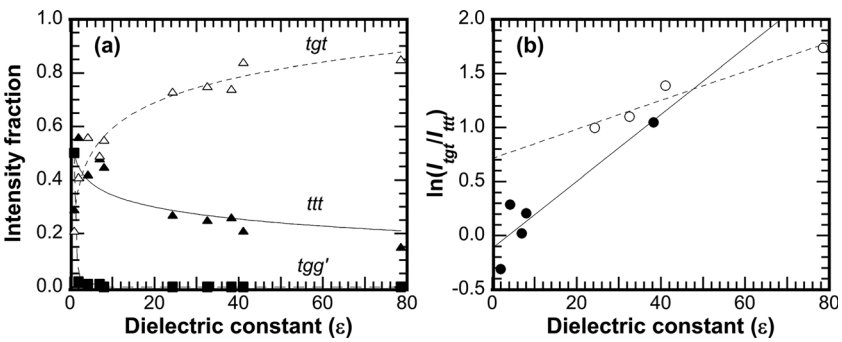

Fig. 5 (a) Dielectric constant (ε) dependence of the intensity fraction of three major conformers, *ttt* (▲), *tgt* (△), and *tgg′* (■). (b) Plot of $\ln(I_{tgt}/I_{ttt})$ *vs.* ε. Hydrogen-bonding (○) and non-hydrogen-bonding solvents (●) are shown with different symbols.

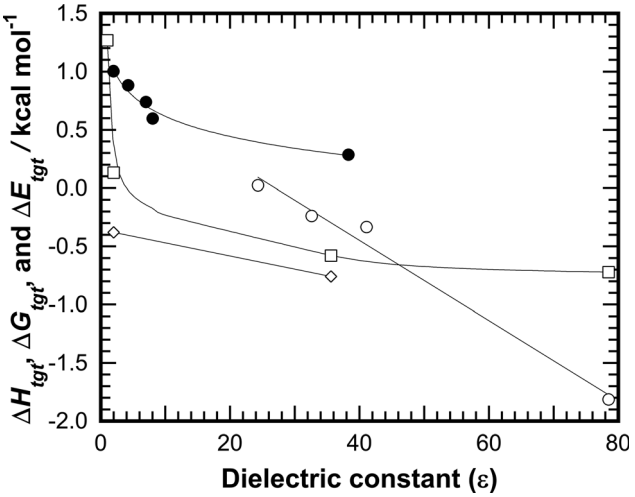

Fig. 6 Energy difference (kcal mol^{-1}) between the *ttt* and *tgt* conformers of DTBE in various solvents: Raman (ΔH_{tgt}: ● and ○), NMR (ΔE_{tgt}: ◇), CCSD(T)/Def2-TZVPPD calculation (ΔG_{tgt}: □). For numerical values, see the 3rd column of Table 3 (Raman), the 2nd column of Table 1 for NMR, and Table 2 for the MO calculation. As for the Raman measurements, following the trend seen in Fig. 5b, the data for non-hydrogen-bonding (●) and hydrogen-bonding solvents (○) are shown with different symbols.

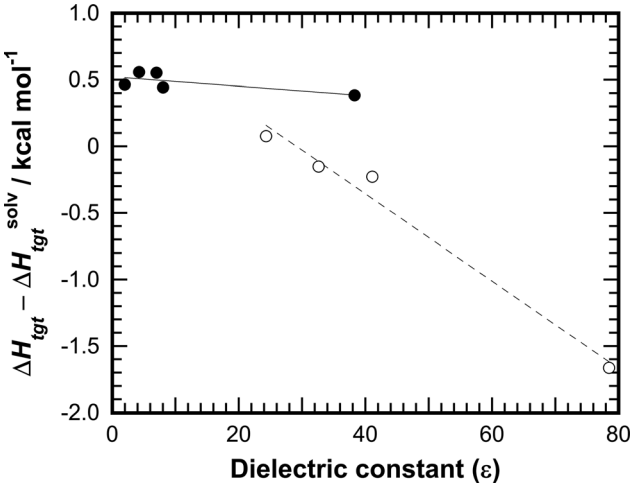

Fig. 7 Plot of the difference, $\Delta H_{tgt} - \Delta H_{tgt}^{solv}$ as a function of ε. Different symbols are used to distinguish the presence (○) or absence (●) of the hydrogen-bonding ability of the given solvents.

There are some differences depending on the method used. While in the Raman spectra each conformer is identified as an isolated peak (Fig. 2), the observed coupling constant from NMR analysis consists of an average of the contributions of the participating conformers (Fig. 3). In Fig. 6, the NMR data (◇) tend to be lower than those (●) obtained by the Raman technique. The plot for the MO calculation falls into the Raman region at ε = 1.0, and then drops rapidly with increasing ε, approaching the NMR range. In common, however, the *tgt* form tends to become more stable as the polarity of the solvent increases. This trend has generally been attributed to differences in the dipole moments of the *ttt* and *tgt* conformations. It may be interesting to note that under the hydrogen-bonding environment such as in ethanol, methanol and water, the Raman observation (○) tends to depart from the theoretical estimation (□).

3-2. Enhancement of the *gauche* stabilization in hydrogen-bonding solvents

The unique behaviors of hydrogen-bonding solvents are noted both in Fig. 5 and 6. To examine some more details, the solvation enthalpies are separately estimated for *ttt* and *tgt* in given solvent systems according to PCM with the integral equation formalism variant (IEFPCM) (B3LYP/6-31G(d,p) basis set). The effect of dielectric media ΔH_{tgt}^{solv} thus estimated is listed in the 4th column of Table 3. By taking the difference between the values in columns 3 and 4, the contribution arising from the polarity of the surrounding solvents may be roughly eliminated. The values derived in this manner are listed in the last column of the same table, and plotted in Fig. 7 against ε of the solvents.

The results shown in Fig. 7 can be divided into two groups. The data in conventional organic solvents free from hydrogen bonding are scattered around a horizontal line (∼0.48 kcal mol^{-1}), whereas the plots for ethanol, methanol, and water form a downward-sloping line. The results of the first group indicate that the contributions from solvents due to the electrostatic and dispersion interactions are reasonably well evaluated by the PCM treatment. Since the contribution from hydrogen-bond formation with solvent molecules is not considered in the PCM calculation, the deviation observed in the second group may be a trend specific to hydrophilic environments. Accordingly, the data points for methanol, ethanol, ethylene glycol and water are shown with open circles. Water is unique in that it has a three-dimensional structure unlike alcoholic solvents, and the straight lines in the diagram have no meaning other than to show that they are the data in hydrogen-bonding solvents.

The discrepancy between the experimental values and the MO theoretical calculations (CCSD(T)/Def2-TZVPPD) in the hydrophilic region of Fig. 6 may suggest that the actual situation of the hydrated structure of DTBE is not appropriately reflected in the basis set used.

3-3. 1,5-Through-space interactions involved in the *tgg′* arrangement

The Raman spectrum shown in Fig. 2 suggests that the *tgg′* conformer (*cf.* Fig. 1c) is the most populated species in the gas phase. The calculated ΔG value (3.0 kcal mol^{-1}) (Table 2) is apparently inconsistent with the observation. The *tgg′* conformer exists only in a trace amount in cyclopentane and is no longer detectable in the neat liquid. Acknowledging some discrepancies between MO calculations and actual measurements, the results of the calculation should still serve as a useful reference for understanding the stability of *tgg′* in the condensed phase.

From the results of the CCSD(T)/Def2-TZVPPD calculation, we may follow the change in the energy state of *tgg′* (*cf.* Table 2) as a function of ε. The 1,5-*t*-Bu···O contact is supposed to be an electrostatic attractive interaction between the *t*-butyl group

and oxygen atom separated by four bonds. More precisely, what stabilizes *tgg′* is thought to be the attractive interaction between positively and negatively charged hydrogens of the *t*-butyl group and oxygen, respectively. Indeed, our QTAIM analysis indicated the presence of some C–H···O nonbonding interactions stabilizing the *tgg′* conformer of DTBE (Fig. S1 of the SI). A similar 1,5-interaction is well-known between the methyl group and oxygen atom in the DME, effectively stabilizing the *tgg′* conformer in the gas phase.[6,19,27–29]

Based on the results of Table 2, the energy state of the *tgg′* conformer relative to the most stable *tgt* can be calculated: 1.8 kcal mol^{-1} in the gas phase (ε = 1), 2.6 kcal mol^{-1} in cyclohexane (ε = 2.02), and further increasing to 3.4 kcal mol^{-1} in acetonitrile (ε = 35.6). In accord with the spectroscopic observations, substitution of the terminal group by the *t*-butyl group leads to suppression of the *tgg′* conformer in the condensed phase. As for DME, on the basis of MO calculations, Freitas[19] noted a similar shift in the stability of two conformers *tgt* and *tgg′* in response to the change in environment from the gas to dimethylsulfoxide. As discussed in the preceding section, the hydrogen-bonding characteristic of water seems not to be taken into account appropriately in the present CCSD(T)/Def2-TZVPPD calculation. Therefore, the estimate of 3.5 kcal mol^{-1} in water, calculated in a similar manner, is unlikely to reflect the reality.

To examine the electronic origin of conformational preferences, a Natural Bond Orbital (NBO) second-order perturbation analysis was performed (Table S1 of the SI). In accord with the results of the QTAIM analysis, the LP(O) → σ*(C–H) donor–acceptor charge-transfer interactions involved in the 1,5-through space C–H···O contacts of *tgg′* are individually modest in DTBE. These findings are consistent with stabilization of *tgg′* arising from the cumulative effect of weak interactions. In the condensed phase (acetonitrile), in addition to the usual solvation (dipole) stabilization, some redistribution of n(O) → σ* interactions also appear to be involved.

3-4. Comparison of DTBE and DME

Here we would like to discuss the effect of terminal group X on the conformational preference of the central C–C bond in the conventional organic solvents and aqueous solution.

Due to its unique properties, DME (X = methyl) has attracted the attention of many research groups. The enthalpy differences (ΔH_{tgt}) between rotamers *tgt* and *ttt* observed using vibrational spectroscopy are reported to be 0.17 in the vapor phase, −0.98 in the neat liquid,[12] and −1.92 in water,[37] with all units being kcal mol^{-1}. According to Matsuura *et al.*[13,38] and Wada *et al.*,[14] the conformer fraction, thus the ΔH_{tgt} value, varies appreciably with the temperature and concentration of DME in water. The energy difference (ΔE_{tgt}) estimated by NMR is reported to be −1.2 kcal mol^{-1} in water at the volume fraction 0.5 v/v.[25]

For DTBE, the accurate value of ΔH_{tgt} in the gas phase remains unknown, but the Raman spectrum of the gas phase shown in Fig. 2 may be used as a reference for estimating approximate values: the intensity fraction I_{tgt}/I_{ttt} is around 0.1, suggesting that the energy state is considerably higher than in the case of DME. From Table 3, the values of ΔH_{tgt} in the neat liquid and water are respectively 0.74 and −1.82 kcal mol^{-1}. Although the *ttt* conformer is more preferred for DTBE in the gas and solutions, the general trend of dielectric effects on ΔH_{tgt} resembles that found for DME. The results of our NBO analysis on DTBE presented in SI (Table S1) suggest that upon transition from the gas to a condensed phase such as acetonitrile, some redistribution of n(O) → σ* interactions take place in addition to the solvation (dipolar) stabilization.

Water is the most extensively studied medium with respect to the hydration behavior of DME. The van der Waals volume[39] of the *t*-butyl group is in the range of 85–90 Å^3 while that of the methyl group is about 27 Å^3. Assuming that the spacer portion connecting both ends occupies 70 Å^3, the molecular volumes of DTBE and DME are 240 Å^3 and 124 Å^3, respectively. The occupancy of hydrophobic groups in the entire volume is 70% and 40% for DTBE and DME, respectively. The presence of bulky substituents such as the *t*-butyl group affects the C–O–C bond angle and the OC–CO dihedral angle, and also changes the charge distribution. While the dipole moment of *ttt* is nil due to its planar conformation, the calculated dipole moment of the *tgt* conformer placed in water is 0.91 and 1.8 D (B3LYP/6-31G(d,p) level), respectively, for DTBE and DME. Although the dipole moment of DTBE is not known, the value calculated above for DME is consistent with the value (1.71 D) conventionally adopted for DME in solution. DTBE is apparently less polar than DME. Despite the sizable difference in hydrophobicity and polarity, DTBE is still soluble in water, suggesting that the EG moiety is strongly incorporated into the surrounding medium through hydrogen bonding.

The *ab initio* MO calculations are also attempted for DME by using the CCSD(T)/Def2-TZVP basis set. The results are summarized in Table 4: to facilitate comparison, the framework of Table 2 for DTBE is followed.

As with DTBE, the hydrogen-bonding capacity of water molecules does not appear to be properly estimated, leading to some overestimation of the ΔG value. Nevertheless, the results of the MO calculations are quite suggestive regarding the role of the terminal group of the molecule. For X = methyl, the relative energies of the *tgg′* state remain in the range from −0.05 to −0.18 kcal mol^{-1} from gas to water (Table 4), being more or less consistent with the Raman observation reported by Yoshida *et al.*[8] (0.31 kcal mol^{-1} in the gas phase), by Kudo *et al.*[37] (−0.47 to −0.18 in organic solvents, and −0.39 in water with all units being in kcal mol^{-1}), and NMR analysis of Furuya

Table 4 Theoretical estimation (CCSD(T)/Def2-TZVPD) of free energy differences ΔG (kcal mol^{-1}) for DME conformers in various solvents. The dielectric constants (ε) of the media are also included

	Gas	Cyclohexane	Acetonitrile	Water
ε	1.0	2.02	35.6	78.5
ttt	0.00	0.00	0.00	0.00
tgt	0.33	−0.01	−0.69	−0.71
tgg′	−0.05	−0.07	−0.18	−0.18

et al.[31] (0.48 in the gas phase, 0.8 in the neat liquid and 1.1 kcal mol^{-1} in water). Whereas for X = *t*-butyl, the MO calculation yields $\Delta H_{tgg'}$ = 2–3 kcal mol^{-1} for similar solvent systems (Table 2), indicating that the attractive through-space 1,5-interation should be almost entirely suppressed. The most contrasting difference between DTBE and DME appears in the stability of their *tgg′* conformers. Needless to say, this is essentially due to the difference in the excluded volume, *i.e.*, the steric effect of the terminal group X.[32] In conclusion, the present work on DTBE clearly indicates that the *gauche* oxygen effect of EG units is not necessarily related to the through-space 1,5-contact involving adjacent C–O bonds.

4. Concluding remarks

The influence of the *gauche* effect on the conformer fraction of 1,2-dihaloethane molecules has been discussed using quantum mechanical methods in terms of the balance between the *gauche* preference due to the hyperconjugative orbital interactions and the steric Pauli repulsion.[40] The *gauche* oxygen effect specific to the EG unit may also involve a similar mechanism. The behavior of DTBE in conventional organic solvents shown in Fig. 6 resembles that of $ClCH_2CH_2Cl$ (DCE) reported in the literature.[41,42] For DCE, the enthalpy difference between the *gauche* and *trans* states decreases as the dielectric constant of the solvent increases. Although the solubility of DCE in water is limited, the enthalpy data from Raman spectroscopy are available in a report by Kato *et al.*[42] They reported that the *trans* form is more stable with the enthalpy gap of 0.63 kcal mol^{-1} in water. In contrast, DTBE is soluble in water with ΔH_{tgt} = −1.82 kcal mol^{-1}, despite having bulky hydrophobic groups at the terminals. The contrasting behavior of these two molecules illustrates an enhanced *gauche* oxygen effect of DTBE through hydrogen-bond formation in water.[13,14,37]

Finally, we would like to point out that in our everyday lives we benefit from the *gauche* oxygen effect not only in POE but also in other polymeric materials. A similar tendency has been reported for the EG units in the well-known polymer poly(ethylene terephthalate) $[-OCH_2CH_2OC(=O)\phi C(=O)-]_n$ (PET) and in its model compounds.[18,43–45] The C–C bond in the EG segment contained in the repeating unit of the PET chain prefers a higher-multiplicity *gauche* conformation rather than the *trans* form in the fluid or amorphous state; upon crystallization, however, it converts to a more efficiently packed *trans* arrangement, even at the expense of a substantial loss of entropy due to the difference in the multiplicity of the two conformations. Without the *gauche* oxygen effect in the EG unit, the melting point of PET resins would increase, melt processing would become more difficult, and the accompanying increase in crystallinity should inevitably impair their transparency.

Conflicts of interest

There are no conflicts of interest to declare.

Data availability

The data supporting this article have been included as part of the supplementary information (SI).

Supplementary information: Results of QTAIM and NBO analyses. See DOI: https://doi.org/10.1039/d5cp04244e.

Acknowledgements

We would like to express our sincere gratitude to Dr Masahide Yamamoto, Professor Emeritus of Kyoto University for his great interest and help in this long-term project. Technical assistance from Dr Susumu Kawauchi and Mr Yoji Kawase in performing the MO calculations is gratefully acknowledged. We also thank Dr Yuji Sasanuma for his valuable comments during the preparation of the article.

References

1 P. J. Flory, *Statistical Mechanics of Chain Molecules*, Interscience, New York, 1969.
2 A. Abe and J. E. Mark, *J. Am. Chem. Soc.*, 1976, **98**, 6468–6476.
3 A. Abe, K. Tasaki and J. E. Mark, *Polym. J.*, 1985, **17**, 883–893.
4 Y. Ogawa, M. Ohta, M. Sakakibara, H. Matsuura, I. Harada and T. Shimanouchi, *Bull. Chem. Soc. Jpn.*, 1977, **50**, 650–660.
5 H. Matsuura and K. Fukuhara, *J. Polym. Sci., Part B: Polym. Phys.*, 1986, **24**, 1383–1400.
6 H. Yoshida, I. Kaneko, H. Matsuura, Y. Ogawa and M. Tasumi, *Chem. Phys. Lett.*, 1992, **196**, 601–606.
7 S. Masatoki, M. Takamura, H. Matsuura, K. Kamogawa and T. Kitagawa, *Chem. Lett.*, 1995, 991–992.
8 H. Yoshida, T. Tanaka and H. Matsuura, *Chem. Lett.*, 1996, 637–638.
9 H. Matsuura and T. Sagawa, *J. Mol. Liq.*, 1995, **65/66**, 313–316.
10 R. Begum and H. Matsuura, *J. Chem. Soc., Faraday Trans.*, 1997, **93**, 3839–3848.
11 H. Yoshida and H. Matsuura, *J. Phys. Chem. A*, 1998, **102**, 2691–2699.
12 N. Goutev, K. Ohno and H. Matsuura, *J. Phys. Chem. A*, 2000, **104**, 9226–9232.
13 A. S. Wahab and H. Matsuura, *J. Mol. Struct.*, 2002, **606**, 35–43.
14 R. Wada, K. Fujimoto and M. Kato, *J. Phys. Chem. B*, 2014, **118**, 12223–12231.
15 G. D. Smith, D. Y. Yoon, R. L. Jaffe, R. H. Colby, R. Krishnamoorti and L. J. Fetters, *Macromolecules*, 1996, **29**, 3462–3469.
16 G. D. Smith, D. Y. Yoon and R. L. Jaffe, *Macromolecules*, 1993, **26**, 5213–5218.
17 A. Abe, H. Furuya, M. K. Mitra and T. Hiejima, *Comput. Theor. Polym. Sci.*, 1998, **8**, 253–258.
18 Y. Sasanuma, *Conformational Analysis of Polymers*, John Wiley & Sons, NJ, 2023.
19 M. P. Freitas, *ChemPhysChem*, 2025, **26**, e202500458.

20 S. Yamaguchi, Y. Morino, I. Watanabe and S. Mizushima, *Sci. Pap. Inst. Phys. Chem. Res.*, 1943, **40**, 417–424.
21 S. Mizushima, *Structure of Molecules and Internal Rotation*, Academic Press, New York, 1954.
22 S. Wolfe, *Acc. Chem. Res.*, 1972, **5**, 102–111.
23 H. Matsuura, T. Miyazawa and K. Machida, *Spectrochim. Acta*, 1973, **29A**, 771–779.
24 V. Viti, P. L. Indovina, F. Podo, L. Radics and G. Némethy, *Mol. Phys.*, 1974, **27**, 541–559.
25 K. Tasaki and A. Abe, *Polm. J.*, 1985, **17**, 641–655.
26 Y. Yokoyama, H. Uekusa and Y. Ohashi, *Chem. Lett.*, 1996, 443–444.
27 E. E. Astrup, *Acta Chim. Scand. A*, 1979, **A33**, 655–664.
28 R. L. Jaffe, G. D. Smith and D. Y. Yoon, *J. Phys. Chem.*, 1993, **97**, 12745–12751: the authors reexamined the NMR gas phase data reported by Inomata and Abe[29] on the basis of their MO calculation and concluded that *tgg′* is the most populated species and *ttt* becomes slightly more stable than *tgt* in opposite to the order in the liquid state.
29 K. Inomata and A. Abe, *J. Phys. Chem.*, 1992, **96**, 7934–7937; the NMR experimental data reported in this article have been recalculated by Furuya and Abe (unpublished) in consideration of the electrostatic through-space 1,5-$CH_3\cdots O$ contact within in the RIS scheme.
30 S. Tsuzuki, T. Uchimaru, K. Tanabe and H. Hirano, *J. Phys. Chem.*, 1993, **97**, 1346–1350.
31 H. Furuya and A. Abe, unpublished: The NMR data reported in ref. 25 have been refined in consideration of the electrostatic through-space 1,5-$CH_3\cdots O$ contact.
32 E. L. Eliel and S. H. Wilen, *Stereochemistry of Organic Compounds*, Wiley, New York, 1994.
33 M. J. Frisch, G. W. Trucks, H. B. Schlegel, G. E. Scuseria, M. A. Robb, J. R. Cheeseman, G. Scalmani, V. Barone, B. Mennucci, G. A. Petersson, H. Nakatsuji, M. Caricato, X. Li, H. P. Hratchian, A. F. Izmaylov, J. Bloino, G. Zheng, J. L. Sonnenberg, M. Hada, M. Ehara, K. Toyota, R. Fukuda, J. Hasegawa, M. Ishida, T. Nakajima, Y. Honda, O. Kitao, H. Nakai, T. Vreven, J. A. Montgomery, Jr., J. E. Peralta, F. Ogliaro, M. Bearpark, J. J. Heyd, E. Brothers, K. N. Kudin, V. N. Staroverov, T. Keith, R. Kobayashi, J. Normand, K. Raghavachari, A. Rendell, J. C. Burant, S. S. Iyengar, J. Tomasi, M. Cossi, N. Rega, J. M. Millam, M. Klene, J. E. Knox, J. B. Cross, V. Bakken, C. Adamo, J. Jaramillo, R. Gomperts, R. E. Stratmann, O. Yazyev, A. J. Austin, R. Cammi, C. Pomelli, J. W. Ochterski, R. L. Martin, K. Morokuma, V. G. Zakrzewski, G. A. Voth, P. Salvador, J. J. Dannenberg, S. Dapprich, A. D. Daniels, O. Farkas, J. B. Foresman, J. V. Ortiz, J. Cioslowski and D. J. Fox, *Gaussian 09, Revision C.01*, Gaussian, Inc., Wallingford CT, 2010.
34 G. D. Purvis III and R. L. Bartlett, *J. Chem. Phys.*, 1982, **76**, 1910–1918.
35 F. J. Weigend, *Chem. Phys.*, 2006, **8**, 1057–1065.
36 J. R. Nestor and E. R. Lippincott, *J. Raman Spectrosc.*, 1973, **1**, 305–318.
37 Y. Kudo, Bachelor's thesis, Department of Applied Chemistry, Faculty of Science and Engineering, Ritsumeikan University, 2005.
38 S. A. Wahab and H. Matsuura, *Chem. Lett.*, 2001, 198–199.
39 A. Bondi, *J. Phys. Chem.*, 1964, **68**, 441–451.
40 D. R. Silva, L. A. Santos, T. A. Hamlin, C. F. Guerra, M. P. Freitas and F. M. Bickelhaupt, *ChemPhysChem*, 2021, **22**, 641–648.
41 R. J. Abraham and E. Bretschneider, in *Internal Rotation in Molecules*, ed. W. J. Orville-Thomas, John Wiley & Sons, Ltd, London, 1974, Table 13.4.
42 M. Kato, M. Abe and Y. Taniguchi, *J. Chem. Phys.*, 1999, **110**, 11982–11986.
43 J. Štokr, B. Schneider, D. Doskočilova, J. Lövy and P. Sedláček, *Polymer*, 1982, **23**, 714–721.
44 S. Pérez and F. Brisse, *Acta Crystallogr.*, 1976, **B32**, 470–474.
45 A. Abe, H. Furuya, T. Hiejima and T. Nishiyama, *Polym. J.*, 2008, **40**, 910–914.